

Ionised carbon and galaxy activity

S. J. Curran

School of Physics, University of New South Wales, Sydney NSW 2052, Australia
e-mail: sjc@phys.unsw.edu.au

ABSTRACT

We investigate the possibility that the decrease in the relative luminosity of the $158\ \mu\text{m}$ [C II] line with the far-infrared luminosity in extragalactic sources stems from a stronger contribution from the heated dust emission in the more distant sources. Due to the flux limited nature of these surveys, the luminosity of the detected objects increases with distance. However, the [C II] luminosity does not climb as steeply as that of the far-infrared, giving the decline in the $L_{\text{[C II]}}/L_{\text{FIR}}$ ratio with L_{FIR} . Investigating this further, we find that the [C II] luminosity exhibits similar drops as measured against the carbon monoxide and radio continuum luminosities. The former may indicate that at higher luminosities a larger fraction of the carbon is locked up in the form of molecules and/or that the CO line radiation also contributes to the cooling, done mainly by the [C II] line at low luminosities. The latter hints at increased activity in these galaxies at greater distances, so we suggest that, in addition to an underlying heating of the dust by a stellar population, there is also heating of the embedded dusty torus by the ultra-violet emission from the active nucleus, resulting in an excess in the far-infrared emission from the more luminous objects.

Key words. galaxies: abundances – galaxies: ISM – galaxies: active – Infrared: galaxies – Radio continuum: galaxies– quasars: emission lines

1. Introduction

The $^2\text{P}_{3/2} \rightarrow ^2\text{P}_{1/2}$ fine-structure line of C^+ , [C II], is believed to be a cooling pathway for the diffuse gas in galaxies (Dalgarno & McCray, 1972). This transition traces photo-dissociation regions (PDRs), where the ultra-violet radiation from young stars dominates the heating of the gas. From this process, the [C II] luminosity may reach up to 1% the total luminosity of the galaxy (Crawford et al., 1985; Stacey et al., 1991; Wright et al., 1991), thus being the most powerful emission line in many galaxies. From a study of 60 normal galaxies with the Long Wavelength Spectrometer (LWS) on-board the Infrared Space Observatory (ISO, Clegg et al. 1996), Malhotra et al. (2001) find that for far-infrared luminosities of $L_{\text{FIR}} \lesssim 10^{11}\ \text{L}_{\odot}$, the $L_{\text{[C II]}}/L_{\text{FIR}}$ ratio is roughly constant at $\log_{10}(L_{\text{[C II]}}/L_{\text{FIR}}) \sim -2.5$, but drops rapidly above these values (Fig. 1). This normalised decrease in the brighter galaxies is attributed to an increased grain charge, lowering the kinetic energy of the liberated photo-electrons which deliver heat to the gas.

Negishi et al. (2001) extended this sample to include starburst galaxies and active galactic nuclei (AGN), all of which are found to follow the same trend, suggesting that far-infrared emission in the active galaxies also arises primarily from star forming activity. Rather than an increase in the charge carried by the dust grains, Negishi et al. (2001) suggest that the $L_{\text{[C II]}}/L_{\text{FIR}}$ decrease with L_{FIR} is due to higher gas densities resulting in higher collision rates, thus de-exciting the ionised carbon through a non-radiative process.

Luhman et al. (1998, 2003) confirm the decrease in $L_{\text{[C II]}}/L_{\text{FIR}}$ with L_{FIR} to higher luminosities ($L_{\text{FIR}} \gtrsim 10^{12}\ \text{L}_{\odot}$), by observing [C II] in a sample of ultra-luminous infrared galaxies (ULIRGs). This trend is in part attributed to much of the far-infrared emission arising from dust-bounded photo-ionised gas which does not contribute to the [C II] emission. Most recently, the far-infrared luminosities have been taken up another notch by the two high redshift detections of [C II], which again follow

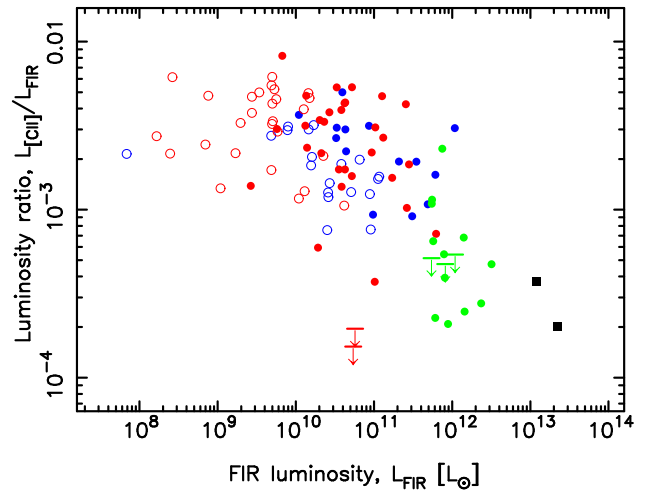


Fig. 1. The $L_{\text{[C II]}}/L_{\text{FIR}}$ ratio versus L_{FIR} for the low redshift ($z \lesssim 0.1296$) galaxies and the high redshift quasar searches (cf. figure 2 of Maiolino et al. 2005). Throughout this paper the symbols are colour coded according to the source reference – red (Malhotra et al., 2001), blue (Negishi et al., 2001), green (Luhman et al., 2003) and black (the two high redshift [C II] detections of Maiolino et al. 2005; Iono et al. 2006). The downwards arrows show the 3σ upper limits. As per Luhman et al. (2003); Maiolino et al. (2005), the hollow symbols indicate where the $\approx 80''$ LWS aperture (Clegg et al. 1996) subtends $\lesssim 10$ kpc and the filled symbols where the aperture subtends $\gtrsim 10$ kpc (at angular diameter distances of $\gtrsim 26$ Mpc or $z \gtrsim 0.006$ – throughout this paper we use $H_0 = 71\ \text{km s}^{-1}\ \text{Mpc}^{-1}$, $\Omega_{\text{matter}} = 0.27$ and $\Omega_{\Lambda} = 0.73$, Spergel et al. 2003).

the same decline in $L_{\text{[C II]}}/L_{\text{FIR}}$ (Maiolino et al., 2005; Iono et al., 2006). Once more, this indicates different excitation conditions

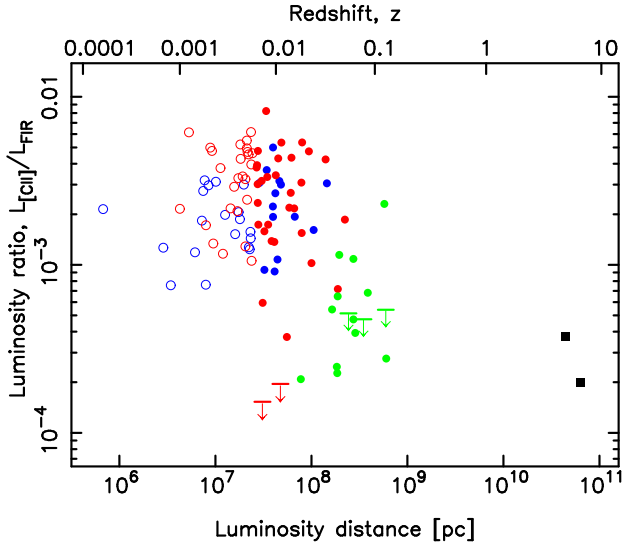


Fig. 2. The $L_{[\text{CII}]} / L_{\text{FIR}}$ ratio versus the luminosity distance. The symbols are as per Fig. 1.

than in local galaxies (Iono et al., 2006) and possibly extremely high star formation rates ($\sim 3000 \text{ M}_{\odot} \text{ yr}^{-1}$, Maiolino et al. 2005) in the early Universe. From all of these studies (summarised in Fig. 1), there is no doubt that the relative strength of the $[\text{C II}]$ line drops with far-infrared luminosity. However, such flux limited surveys are subject to a selection effect, where only the brighter sources are detected at large distances. It is therefore possible that the $[\text{C II}]$ deficit is caused by changing demographics of the galaxies at larger distances, a possibility we investigate in this paper.

2. Possible selection effects

2.1. Relative $[\text{C II}]$ luminosities

In Fig. 2 we replot the $[\text{C II}]$ –FIR luminosity ratio against the luminosity distance (cf. Fig. 1), from which we find a very similar trend. Using Kendall’s τ rank correlation coefficient, which is a non-parametric test of the degree of correspondence between two parameters, we find a 0.009 probability that there is no correlation between the $L_{[\text{CII}]} / L_{\text{FIR}}$ ratio and distance (Table 1¹). This decreases to $P(\tau) = 0.002$ for the LWS “point” sources (i.e. those at $z > 0.006$), where the $[\text{C II}]$ emission should be fully sampled. If the $L_{[\text{CII}]} / L_{\text{FIR}}$ ratio and the distance are unrelated, a 0.2% probability would be located at 3.06σ on the tails of a normalised Gaussian (mean = 0, $\sigma = 1$), suggesting that there is a correlation.

Clearly, there exists the possibility that the correlation is dominated by the inclusion of the two high-redshift quasars ($z = 6.42$, Maiolino et al. 2005 and $z = 4.69$, Iono et al. 2006, cf. $z \leq 0.1296$ for the rest of the sample). Excluding these from the statistics, however, we see that a correlation remains at a

¹ In Table 1 the upper limits are incorporated according to the survival analysis of Isobe et al. (1986), via the ASURV package. This gives Kendall’s τ two-sided probability that there is no correlation between the two ranks, $P(\tau)$, and the subsequent significance of the correlation, $S(\tau)$. Note that where $n = 108$, we have had to exclude the two blue-shifted galaxies (NGC 1569; Malhotra et al. 2001 and Maffei 2; Negishi et al. 2001), since the tested parameters must be converted to log values to run ASURV. With $L_{[\text{CII}]} / L_{\text{FIR}} \gtrsim 10^{-3}$, these occupy the same regions as the other $z < 0.006$ points and do not weaken the correlations.

Table 1. Sample statistics for various redshift ranges – (1) the whole sample, (2) the sources for which the LWS aperture subtends $\gtrsim 10$ kpc, (3) also excluding the two high-redshift quasars (Maiolino et al., 2005; Iono et al., 2006) and finally, (4) the sources for which the aperture subtends $\lesssim 10$ kpc.

Redshift range	n	$P(\tau)$	$S(\tau)$
$L_{[\text{CII}]} / L_{\text{FIR}}$ –Luminosity distance (Fig. 2)			
Whole	108	0.0090	2.61σ
$z > 0.006$	63	0.0022	3.06σ
$0.006 \leq z \leq 0.1296$	61	0.0114	2.53σ
$0 < z \leq 0.006$	45	0.1589	1.41σ
$L_{[\text{CII}]} - L_{\text{FIR}}$ (Fig. 3)			
Whole	110	5.9×10^{-30}	11.4σ
$z > 0.006$	63	1.1×10^{-14}	7.73σ
$0.006 < z \leq 0.1296$	61	1.8×10^{-13}	7.36σ
$0 < z \leq 0.006$	45	5.2×10^{-13}	7.22σ
$L_{[\text{CII}]}$ –Luminosity distance (Fig. 4)			
Whole	108	1.1×10^{-19}	9.08σ
$z > 0.006$	63	4.1×10^{-10}	6.25σ
$0.006 < z \leq 0.1296$	61	6.6×10^{-9}	5.80σ
$0 < z \leq 0.006$	45	0.0060	2.75σ
L_{FIR} –Luminosity distance (Fig. 4)			
Whole	108	2.3×10^{-19}	9.00σ
$z > 0.006$	63	8.1×10^{-13}	7.16σ
$0.006 < z \leq 0.1296$	61	1.6×10^{-11}	6.74σ
$0 < z \leq 0.006$	45	0.1152	1.58σ

2.53σ significance. Finally, note that at $z = 0.0072$ and 0.011 , the two non-detections of Malhotra et al. (2001), which are the only two significant outliers (as they are for the $L_{[\text{CII}]} / L_{\text{FIR}}$ versus L_{FIR} correlation, Fig. 1), lie close to the $z = 0.006$ “beam-filling” cut-off. At these respective redshifts, the $< 80''$ LWS beam (Negishi et al., 2001) subtends < 11 and < 17 kpc and so these may not represent true $L_{[\text{CII}]}$ upper limits (although cf. Fig. 3). The exclusion of these sources raises the significances to 2.89σ (whole sample) and 3.74σ ($z > 0.006$). We include these in Table 1, however, as per the other authors, we use a cut-off of 10 kpc for the diameter of the LWS beam. Finally, there is also the possibility of an undetected population of objects with large $L_{[\text{CII}]} / L_{\text{FIR}}$ ratios at large distances (i.e. located to the top right of Fig. 2). If there is a population of faint sources at large distances, their effect on Fig. 1 would have to be considered, although these would suggest that the decline in $L_{[\text{CII}]} / L_{\text{FIR}}$ with luminosity distance is a selection effect, introduced by the flux limited nature of the surveys. Caution must therefore be advised in interpreting Fig. 1 and the following figures, as it is possible that the locus of points may actually represent the upper luminosity edge of a wedge of undetected lower luminosity sources.

Fig. 3 shows the $[\text{C II}]$ versus the FIR luminosity, which appear to be closely correlated over the whole range of luminosities (Table 1). Note, however, that with a gradient of less than unity (0.77 ± 0.03 , incorporating the upper limits), the least-squares fit to these data demonstrates that $L_{[\text{CII}]}$ does not match the climb in L_{FIR} , confirming a depletion in the $[\text{C II}]$ luminosity in relation to the FIR emission. This is further illustrated in Fig. 4, where the increase in both $L_{[\text{CII}]}$ and L_{FIR} with distance is due to the increase in the lower limit of the luminosities which can be detected. The figure confirms that $L_{[\text{CII}]}$ does not climb quite so

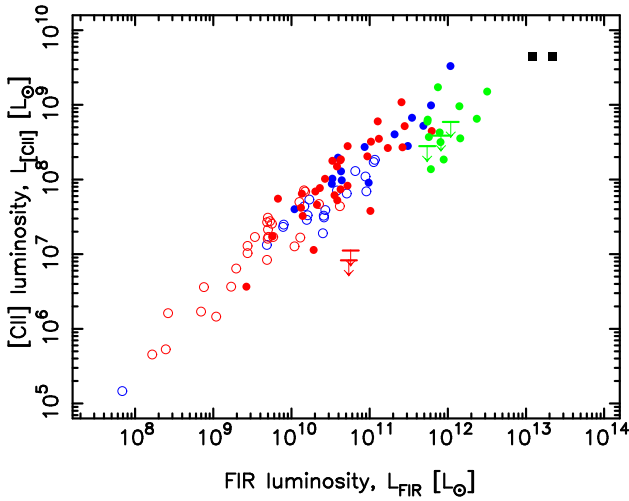


Fig. 3. The [C II] luminosity versus the FIR luminosity.

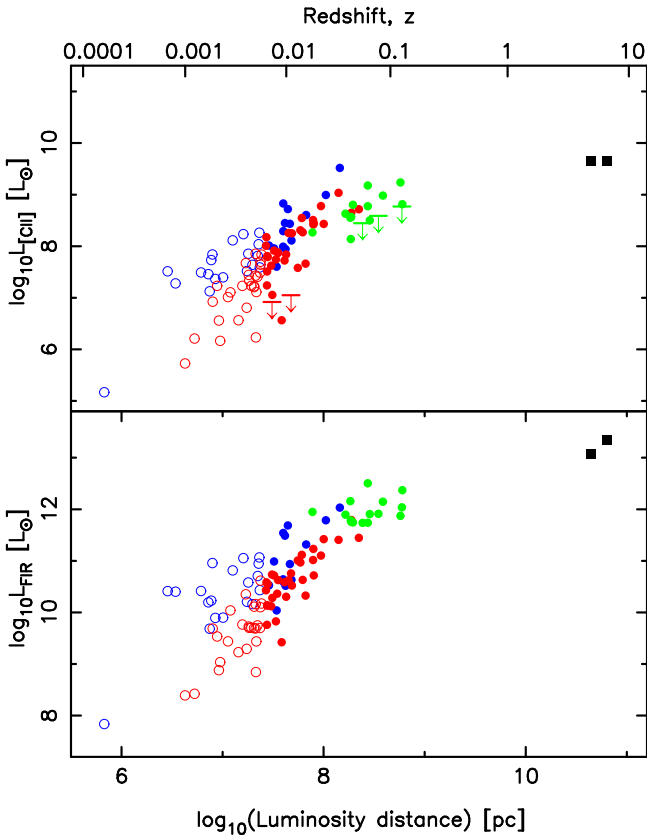


Fig. 4. The [C II] and FIR luminosities versus the luminosity distance. The least-squares fit to $\log_{10} L_{\text{CII}} - \log_{10}(\text{luminosity distance})$ has a gradient of 0.89 ± 0.07 (incorporating the upper limits) and the fit to $\log_{10} L_{\text{FIR}} - \log_{10}(\text{luminosity distance})$ has a gradient of 1.16 ± 0.08 , over the whole redshift range. The panels are plotted to cover the same luminosity range (in decades), from which we see a clear deficit in L_{CII} in comparison to L_{FIR} as the distances increase.

rapidly as L_{FIR} , with an apparent slowing in the increase of L_{CII} at $\geq 10^8$ pc, where the ULIRGs dominate. This indicates that the $L_{\text{CII}}/L_{\text{FIR}}$ –luminosity distance trend (Fig. 2) is the result of lower relative L_{CII} contribution at larger distances and that the anti-correlation is not purely due to the two high redshift points.

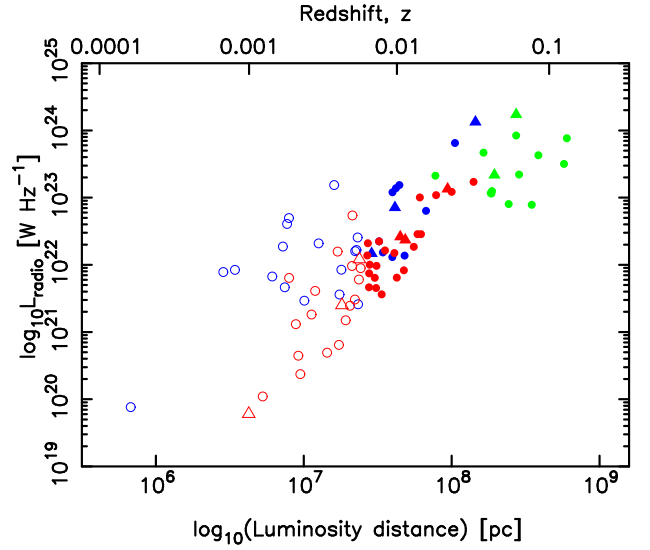


Fig. 5. The 1.4 GHz continuum luminosity versus the luminosity distance. We show this up to $z \sim 0.13$, since there are no radio flux measurements available for the two high redshift sources. The triangles designate fluxes interpolated from neighbouring radio frequencies. Note that the top right corner is within the realm of radio galaxies and quasars where luminosities of $L_{\text{radio}} \geq 10^{24}$ W Hz $^{-1}$ are found at $z \geq 0.1$ (see figure 4 of Curran et al. 2008.)

2.2. Possible causes

2.2.1. Increasing AGN activity

Even with the exclusion of the two high redshift quasars the redshift range spanned by the sample is considerable, with $z \leq 0.1296$ corresponding to a luminosity distance of ≤ 600 Mpc, or looking back 12% into the history of the Universe. At these moderate redshifts, we may expect a change in the demographics of the galaxies from those in the local Universe, as is seen from the presence of the ULIRGs (above) or a larger population of AGN (see below). In fact, among a list of scenarios possibly responsible for the decline in $L_{\text{CII}}/L_{\text{FIR}}$, Malhotra et al. (2001) have suggested that increased AGN activity, over and above that of the starburst, could be the cause of the changing $L_{\text{CII}}/L_{\text{FIR}}$ ratios.

AGN activity may be traced by radio loudness, with radio surveys at 1.4 GHz finding a bimodal distribution in the brightness of extragalactic radio sources: The vast majority of the radio-loud (over 95% with $S_{\text{radio}} \geq 50$ mJy) being radio galaxies and quasars, whereas the radio-quiet tend to be star-forming galaxies (which dominate at flux densities of $S_{\text{radio}} \lesssim 1$ mJy, Condon 1984; Windhorst et al. 1985). We have therefore trawled the NASA/IPAC Extragalactic Database (NED) for the 1.4 GHz flux densities of the galaxies searched for in [C II] and converted these to radio luminosities, which we show in Fig. 5. As seen from this (and Table 2), there is a very strong correlation between radio luminosity and distance. Again, this is not surprising due to the flux limited nature of these surveys, but it does show that even over the low redshift sample ($z \leq 0.1296$), there is a strong selection effect.

Along with the distinct differences in radio fluxes, there is a difference in the redshift distributions, with the AGN exhibiting the higher values (Condon, 1984). This is confirmed by the 2dF and 6dF Galaxy Redshift Surveys (Sadler et al. 1999; Mauch & Sadler 2007), where star-forming galaxies have a me-

dian redshift of $z \approx 0.05$, in contrast to $z \approx 0.1$ for the AGN, which also exhibit a longer high redshift tail (up to the $z = 0.3$ limit of the surveys)². Over the range of this sample ($z \leq 0.1296$), the vast majority of star forming galaxies in the 2dF sample have radio luminosities of $L_{\text{radio}} \lesssim 10^{23} \text{ W Hz}^{-1}$, with most AGN kicking in at $z \gtrsim 0.1$ with $L_{\text{radio}} \gtrsim 10^{23} \text{ W Hz}^{-1}$ (Sadler et al., 1999)³. Note that for the latter this value is close to the radio flux limit, and so a more radio-faint AGN population at high redshift cannot be ruled out. However, 87 of the 108 sources have published (and detected) radio fluxes, where radio loudness is not necessarily a prerequisite for far-infrared selected surveys⁴, although ionised gas will emit a radio continuum (see Negishi et al. 2001). As well as the possibility of a faint AGN population, there are expected to be higher redshift star forming galaxies, but by $z \approx 0.2$, these are already below the $\sim \text{mJy}$ detection threshold. As stated above, most of the [C II] sample is detected in the radio, due in part to the generally low redshifts, and in Fig. 6 we show the [C II] and FIR luminosities against that of the radio.

From this, we see that [C II] luminosity does not climb as steeply as that of the FIR with radio luminosity, which is clearly apparent even with the exclusion of the two high redshift sources (cf. Fig. 4). Rather than heating by stars, the correlation of L_{FIR} with L_{radio} may suggest a significant AGN contribution, where much of the FIR emission may arise from dust heated by ultra-violet emission from the central accretion disk. This is also suspected to be the case in a sample of low redshift Seyfert galaxies, where the FIR emission does not wholly trace the dense star-forming molecular cores (Curran et al., 2001a,c). In extreme cases ($L_{\text{UV}} \gtrsim 10^{23} \text{ W Hz}^{-1}$), high ultra-violet fluxes may be responsible for ionising much of the neutral gas (Curran et al., 2008), making star formation, ironically enough, less likely in the most UV bright sources. Note finally that, although there are no radio fluxes available for the two high redshift [C II] detections, the presence of a powerful X-ray flux from the quasar is invoked by Maiolino et al. (2005) to account for the large populations in the high CO rotational levels at $z = 6.42$, which cannot be obtained from a PDR model of a typical star forming region alone.

2.2.2. Decreasing metallicities

As mentioned above, the galaxies searched probe the past 12% of the Universe, with the two high redshift detections providing end-points at look-back times of 12.4 and 12.8 Gyr, i.e. within the first 12% of the Universe's lifetime. An evolutionary effect, which may give the observed decrease in the [C II] line emission fraction, could be the cosmological evolution of heavy element abundances. A correlation between metallicity and look-back time has already been observed in damped Lyman- α absorption systems over the first 6 Gyr history of the Universe (Prochaska et al., 2003; Curran et al., 2004), and an increase in the carbon abundance with cosmic time could explain the lower

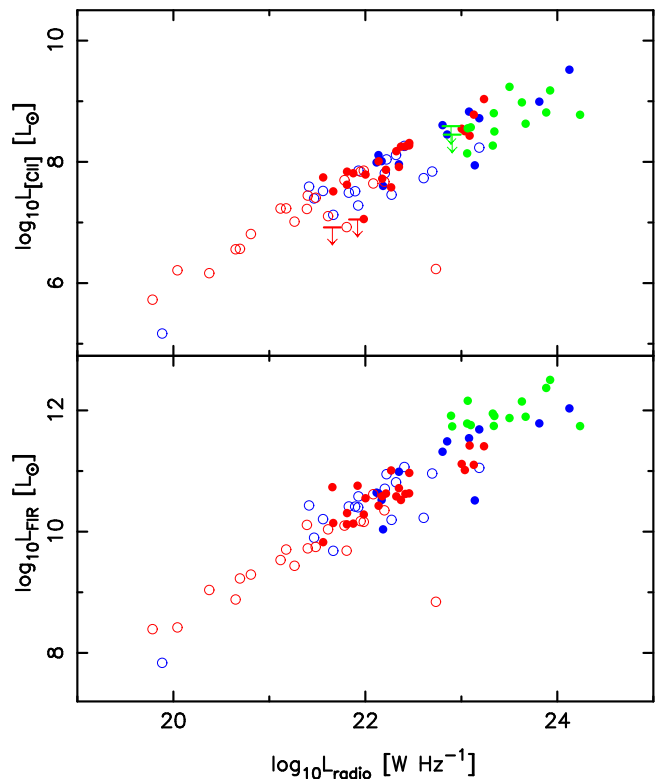


Fig. 6. The [C II] and FIR luminosities versus the 1.4 GHz continuum luminosity. The least-squares fit to $\log_{10} L_{\text{CII}} - \log_{10} L_{\text{radio}}$ has a gradient of 0.77 ± 0.04 (incorporating the upper limits) and the fit to $\log_{10} L_{\text{FIR}} - \log_{10} L_{\text{radio}}$ has a gradient of 0.92 ± 0.05 , over the whole radio luminosity range. As per Fig. 4, the ordinate in both panels are plotted to cover the same luminosity range (in decades).

relative [C II] contribution with increasing redshift (at least over the full $0 < z < 6.42$). A local low metallicity laboratory is the Magellanic clouds, and in the 30 Doradus region of the LMC, Stacey et al. (1991) find [C II]/CO intensity ratios ≈ 30 times larger than Galactic values, later confirmed to be a factor of ≈ 20 over the main part of the LMC ($\approx 6 \times 10 \text{ kpc}^2$, Mochizuki et al. 1994). This is interpreted as the lower metallicities yielding lower dust abundances⁵ and thus providing less shielding from ultra-violet photons, dissociating and ionising the CO into [C II]. In this model the high [C II]/CO ratios are therefore indicative of low metallicities.

Plotting the [C II] and FIR luminosities against that of CO (Fig. 7), we see that both are strongly correlated with this tracer of molecular gas abundance (Table 2) and, again, the [C II] luminosity does not climb as rapidly as L_{FIR} with increasing L_{CO} . Over this wide range of luminosities (and redshifts), there is no large change in the $L_{\text{CII}} - L_{\text{CO}}$ ratio apparent: From a recent survey of the LMC, Bolatto et al. (2000) detect more extended CO emission, undetected by Mochizuki et al. (1994), the contribution of which brings the $L_{\text{CII}}/L_{\text{CO}}$ ratio close to Galactic values. Further afield, Madden et al. (1997) find widely varying $L_{\text{CII}}/L_{\text{CO}}$ ratios in the low-metallicity dwarf galaxy IC 10 and Smith & Madden (1997) find in two spiral galaxies $L_{\text{CII}}/L_{\text{CO}}$ ratios which are an order of magnitude higher than Galactic disk values and more typical of the values found in irregular (low

² Note also, from X-ray photometry Zheng et al. (2004) find that the galaxy population drops at $z \gtrsim 1$, in comparison to $z \gtrsim 2$ for type-2 AGN and no significant redshift dependence for type-1 AGN. From rest-frame UV photometry, Curran et al. (2008) also suspect that all optical+radio bright sources at $z \gtrsim 3$ are type-1 AGN.

³ The range of radio luminosities found may suggest a range of ≈ 0.07 to $\approx 0.3 \times 10^9 M_{\odot}$ for the masses of the central black holes powering the galaxies (Metcalf & Magliocchetti, 2006), over luminosity distances of $\sim 10^7$ to $\sim 10^9 \text{ pc}$ (Fig. 5).

⁴ Malhotra et al. (2001) and Negishi et al. (2001) select near-by normal star-forming galaxies and Luhman et al. (2003) select ULIRGs.

⁵ Such a correlation has been noted at high redshift by Curran et al. (2004).

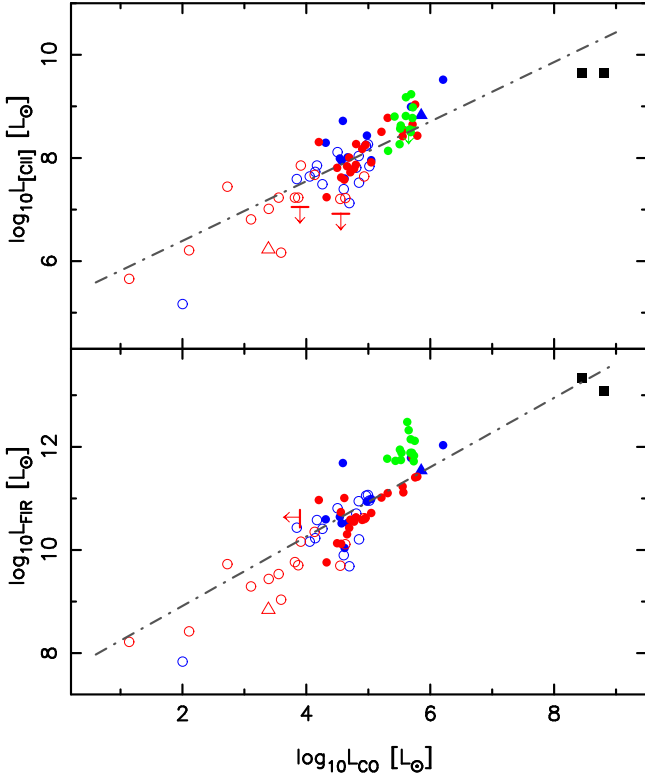


Fig. 7. The [C II] and FIR luminosities versus the CO luminosities, which have been compiled from Sanders & Mirabel (1985); Sanders et al. (1986, 1988, 1991); Solomon & Sage (1988); Heckman et al. (1989); Wiklind & Henkel (1989); Sargent et al. (1989); Eckart et al. (1990); Lees et al. (1991); Tacconi et al. (1991); Claussen & Sahai (1992); Sage (1993); Aalto et al. (1995); Young et al. (1995); Greve et al. (1996); Elfhag et al. (1996); Omont et al. (1996); Solomon et al. (1997); Gao & Solomon (1999); Curran et al. (2001b); Boselli et al. (2002); de Mello et al. (2002); Bertoldi et al. (2003); Yao et al. (2003); Strong et al. (2004); Leroy et al. (2005); Albrecht et al. (2007). The shapes designate the CO rotational transition; circles – $J = 1 \rightarrow 0$, triangles – $J = 2 \rightarrow 1$ and the squares the higher CO transitions for the two high redshift [C II] detections. The lines show the least-squares fits to all of the points, in which $\log_{10} L_{\text{CII}} - \log_{10} L_{\text{CO}}$ has a gradient of 0.54 ± 0.05 and $\log_{10} L_{\text{FIR}} - \log_{10} L_{\text{CO}}$ a gradient of 0.67 ± 0.05 .

metallicity) galaxies. This calls into question the effectiveness of this ratio as a tracer of heavy element abundance (although see Bolatto et al. 1999; Röllig et al. 2006).

2.2.3. Star formation rates

A correlation between the [C II] and CO intensities has previously been noted by Stacey et al. (1991), leading to the hypothesis that the ionised carbon and carbon monoxide are spatially coincident. Aalto et al. (1995) suggested that the CO must be reasonably excited (so that $I_{\text{CO } 2 \rightarrow 1} / I_{\text{CO } 1 \rightarrow 0} \gtrsim 0.8$) if associated with a PDR and demonstrated that such CO intensity ratios were satisfied for [C II]/CO $\gtrsim 4000$ in a sample of 19 normal and starburst galaxies. It therefore appears that large $L_{\text{CII}}/L_{\text{CO}}$ ratios are indicative of enhanced star formation (Stacey et al. 1991, see also Bolatto et al. 2000) and, from a sample of 21 late-type galaxies, Pierini et al. (1999) find that $L_{\text{CII}}/L_{\text{CO}}$ is proportional to the star-formation rate in non-starburst galaxies. Furthermore,

Table 2. As per Table 1.

Redshift range	n	$P(\tau)$	$S(\tau)$
$L_{\text{radio}} - \text{Luminosity distance (Fig. 5)}$			
Whole	87	9.7×10^{-16}	8.03σ
$0.006 \leq z \leq 0.1296$	50	3.6×10^{-10}	6.27σ
$0 < z \leq 0.006$	37	0.0891	1.70σ
$L_{\text{CII}} - L_{\text{radio}}$ (Fig. 6)			
Whole	87	1.9×10^{-23}	9.98σ
$0.006 < z \leq 0.1296$	50	7.5×10^{-13}	7.17σ
$0 < z \leq 0.006$	37	2.9×10^{-8}	5.55σ
$L_{\text{FIR}} - L_{\text{radio}}$ (Fig. 6)			
Whole	87	5.5×10^{-24}	10.1σ
$0.006 < z \leq 0.1296$	50	1.3×10^{-11}	6.77σ
$0 < z \leq 0.006$	37	1.1×10^{-8}	5.72σ
$L_{\text{CII}} - L_{\text{CO}}$ (Fig. 7)			
Whole	80	9.4×10^{-19}	8.84σ
$z > 0.006$	49	1.6×10^{-10}	6.40σ
$0.006 < z \leq 0.1296$	47	3.0×10^{-9}	5.93σ
$0 < z \leq 0.006$	30	0.000055	4.03σ
$L_{\text{FIR}} - L_{\text{CO}}$ (Fig. 7)			
Whole	80	1.4×10^{-20}	9.03σ
$z > 0.006$	49	2.8×10^{-10}	6.31σ
$0.006 < z \leq 0.1296$	47	4.6×10^{-9}	5.86σ
$0 < z \leq 0.006$	30	1.3×10^{-6}	4.84σ

Stacey et al. (1991) suggest that starburst galaxies and star forming regions have ratios of $[\text{C II}]/\text{CO} \approx 6000$, three times higher than for quiescent Galactic regions and non-starburst galaxies. In Fig. 7, apart from the $z \lesssim 0.006$ scatter and possibly the ULIRGs, we see no major deviations from the $L_{\text{CII}}/L_{\text{CO}}$ trend, although the log plot will be quite insensitive to a factor of three. It is clear, however, that the ULIRGs have systematically higher $L_{\text{FIR}}/L_{\text{CO}}$ ratios than the rest of the sample, perhaps indicating a contribution to the FIR luminosity from an AGN in addition to that from the heating by stars. Note that Curran et al. (2001c) and Gao & Solomon (2004) find $L_{\text{FIR}} \propto L_{\text{HCN}}$ over three orders of magnitude of luminosity, including the ULIRGs. This suggests that, while the CO traces all of the molecular gas, the HCN, which traces the dense gas, is closely associated with the FIR emission, be this due to star formation and/or AGN activity (Curran et al., 2001c).

2.2.4. Gas cooling by [O I]

In increased far ultra-violet fields the efficiency of the photo-ejection of electrons from dust grains is reduced, whereas the FIR dust emission continues to increase linearly. We may therefore expect the observed relative decline in the [C II] luminosities with those of the FIR. However, since the increased luminosities may also be tracing different galaxy types, we may also expect different contributions from other line coolants. The other major coolant in galaxies is that of the [O I] line, which we show against the [C II] and FIR luminosities in Fig. 8, where again we see a relative decline in L_{CII} . A constant $L_{\text{OI}}/L_{\text{FIR}}$ ratio with L_{FIR} was previously noted by Malhotra et al. (2001); Negishi et al. (2001), which is interpreted as an increase in dust, and therefore gas, temperatures due to a higher incident far ultra-violet flux

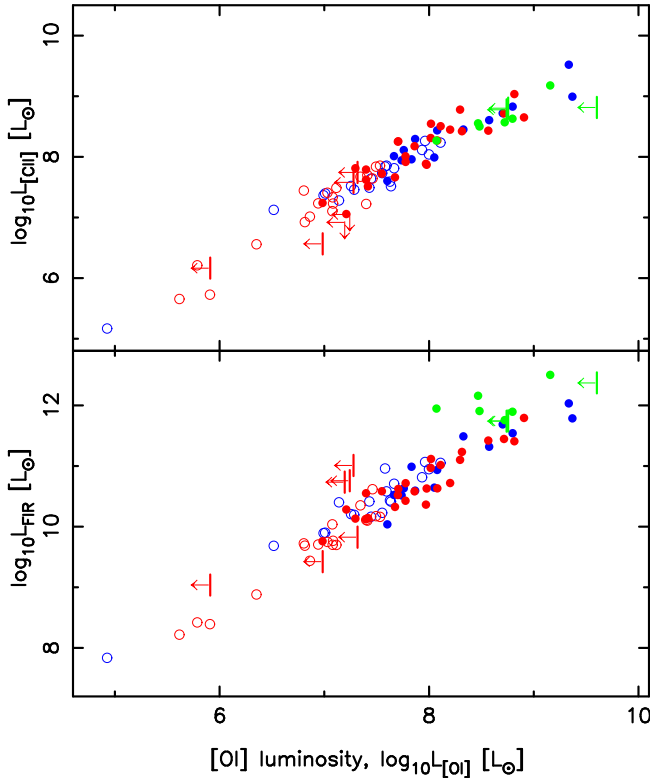


Fig. 8. The [C II] and FIR luminosities versus the [O I] luminosity. The least-squares fit to $\log_{10} L_{\text{CII}} - \log_{10} L_{\text{OI}}$ has a gradient of 0.87 ± 0.05 (incorporating the upper limits) and the fit to $\log_{10} L_{\text{FIR}} - \log_{10} L_{\text{OI}}$ has a gradient of 1.05 ± 0.08 , for $z > 0.006$. As per Fig. 4, the ordinate in both panels are plotted to cover the same luminosity range (in decades).

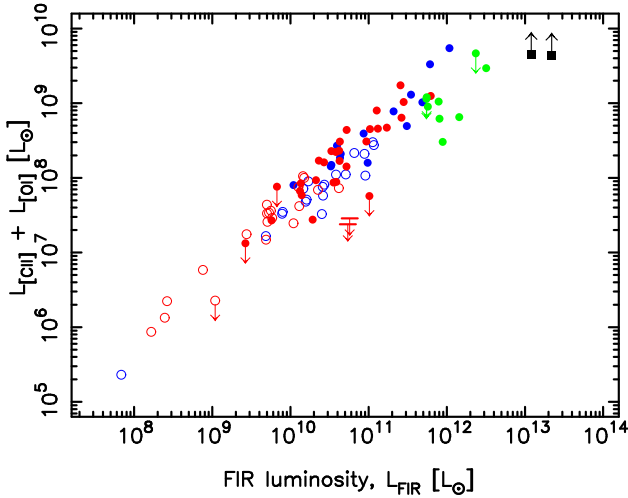


Fig. 9. The [C II] + [O I] luminosity versus the FIR luminosity.

(Kaufman et al., 1999). Again, we see that the FIR luminosities cause the ULIRGs to stray from the lower luminosity trend, although the overall [C II]–[O I] correlation holds tightly for these objects. As for the radio continuum (Fig. 6) and molecular line (Fig. 7) emission, this indicates that there is an excess of FIR emission at higher luminosities.

Lastly, in Fig. 9 we show the total coolant line luminosity (cf. Malhotra et al. 2001) versus that of the far-infrared. The least-squares fit over the whole redshift range has a gradient of

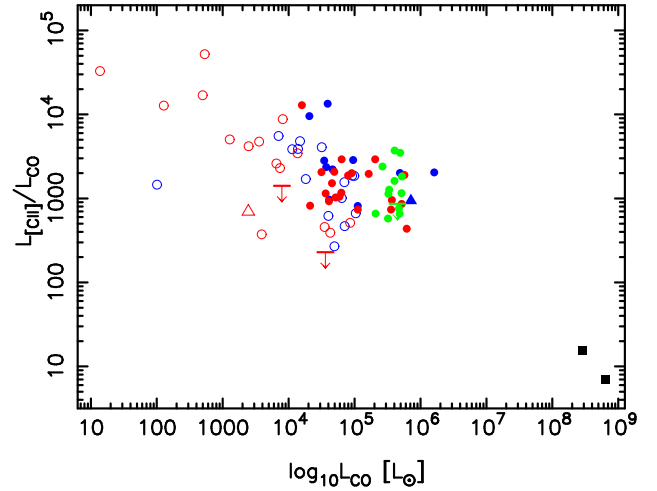


Fig. 10. As Fig. 1, but normalising by the CO luminosity.

0.87 ± 0.03 , which is higher than for the $L_{\text{CII}} - L_{\text{FIR}}$ correlation (0.77 ± 0.03 , Fig. 3), although lower than for $L_{\text{OI}} - L_{\text{FIR}}$ (0.95 ± 0.08 , Fig. 8). This indicates that the [O I] increases its contribution to the cooling of the gas with increasing luminosity and that the stifled [C II] luminosity has the effect of damping the total coolant line luminosity increase in relation to the FIR. This could be partly responsible for the ULIRGs which are, once again, offset from the overall trend, although, as seen in Fig. 8, there is also an FIR excess in relation to the [O I]. Detections of the [O I] emission in the two high redshift objects could verify this trend at the highest luminosities.

Table 3. As per Table 1.

Redshift range	n	$P(\tau)$	$S(\tau)$
$L_{\text{CII}} - L_{\text{OI}}$ (Fig. 8)			
Whole	94	8.3×10^{-31}	11.54σ
$0.006 < z \leq 0.1296$	54	5.1×10^{-16}	8.11σ
$0 < z \leq 0.006$	40	1.2×10^{-12}	7.11σ
$L_{\text{FIR}} - L_{\text{OI}}$ (Fig. 8)			
Whole	94	7.8×10^{-26}	10.51σ
$0.006 < z \leq 0.1296$	54	8.5×10^{-12}	6.83σ
$0 < z \leq 0.006$	40	4.5×10^{-13}	7.24σ
$(L_{\text{CII}} + L_{\text{OI}}) - L_{\text{FIR}}$ (Fig. 9)			
Whole	96	5.1×10^{-26}	10.55σ
$z > 0.006$	56	1.1×10^{-12}	7.12σ
$0.006 < z \leq 0.1296$	54	1.8×10^{-11}	6.72σ
$0 < z \leq 0.006$	40	2.8×10^{-12}	6.99σ

2.3. Recap of the correlations

Here we replot the correlations in the same manner as Fig. 1, where we see similar trends as for $L_{\text{CII}}/L_{\text{FIR}} - L_{\text{FIR}}$: With the inclusion of the two high redshift points, the $L_{\text{CII}}/L_{\text{CO}} - L_{\text{CO}}$ relation (Fig. 10) exhibits the steepest drop (four decades, cf. the not-quite two of the FIR, Fig. 1). Since a significant contribution to this decline is due to the two end points, this may reaffirm our belief that $L_{\text{CII}}/L_{\text{CO}}$ is a poor tracer of metallicity,

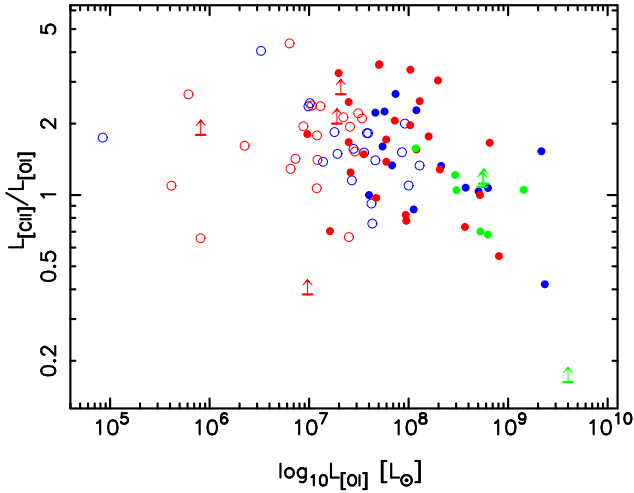


Fig. 11. As above, but normalising by the [O I] luminosity.

since we would expect the highest ratios (lowest metallicities) for the high redshift sources (Sect. 2.2.2). What Fig. 10 suggests, naturally enough, is that the abundance of ionised carbon decreases as more carbon is locked up in molecules, confirming that the two phases share the same location (Stacey et al., 1991) and that the star formation rate may decrease with increasing L_{CO} (Stacey et al., 1991; Pierini et al., 1999; Bolatto et al., 2000).

The presence of molecular gas requires the presence of dust, the heating of which will be responsible for the corresponding drop in $L_{\text{[CII]}}/L_{\text{FIR}}$ with L_{FIR} . However, the changing galactic demographics, due to the necessarily brighter sources at larger luminosity distances, may have differing cooling mechanisms than for the more proximate (and therefore dimmer) examples: The $63 \mu\text{m}$ [O I] line has the effect of increasing the gradient of the coolant line ([C II] + [O I]) luminosity (cf. $L_{\text{[CII]}}$ only) against L_{FIR} and in Fig. 11 we also see a decrease in $L_{\text{[CII]}}/L_{\text{[OI]}}$ with $L_{\text{[OI]}}$. In addition to this, Papadopoulos et al. (2007) suggest that the excited ($J = 4 \rightarrow 3$ & $6 \rightarrow 5$, i.e. $\lambda = 651$ & $434 \mu\text{m}$) CO lines contribute as much to the cooling as the [C II] line in one of the ULIRGs (Mrk 231). From Fig. 10 there is undoubtedly a steep increase in the relative CO luminosity, although it is generally the $J = 1 \rightarrow 0$ transition which has been detected in the ULIRGs and, again, these exhibit an excess in FIR luminosity (see Fig. 7)⁶. Note, however, that for the quasars, where the high excitation transitions are redshifted into more “observer friendly” bands, the $J = 6 \rightarrow 5$ & $7 \rightarrow 6$ ($\lambda = 434$ & $389 \mu\text{m}$) CO luminosities do follow the general trend (Fig. 7).

The clear drop in $L_{\text{[CII]}}/L_{\text{radio}}$ with L_{radio} (Fig. 12), supports the possibility of a changing AGN contribution. As discussed above, star forming galaxies tend to be objects of low radio flux, whereas active galaxies give rise to large radio fluxes and those of our sample, towards the high end, certainly qualify as radio-loud. Quasars, or at least QSOs, are often associated with substantial dust emission (e.g. Smail et al. 1997; Barvainis & Ivison 2002; Cowie et al. 2002), as well as bright CO emission at high redshift (see Hainline et al. 2004 and references therein). Again this raises the possibility that the more radio luminous sources may radiate the excess heat from the AGN through CO emission. Whatever the cause, arguments involving the relative decrease of $L_{\text{[CII]}}$ with L_{FIR} (Malhotra et al., 2001; Negishi et al., 2001;

⁶ Also, Papadopoulos et al. (2007) believe that the lower rotational transitions do not trace the same gas phase.

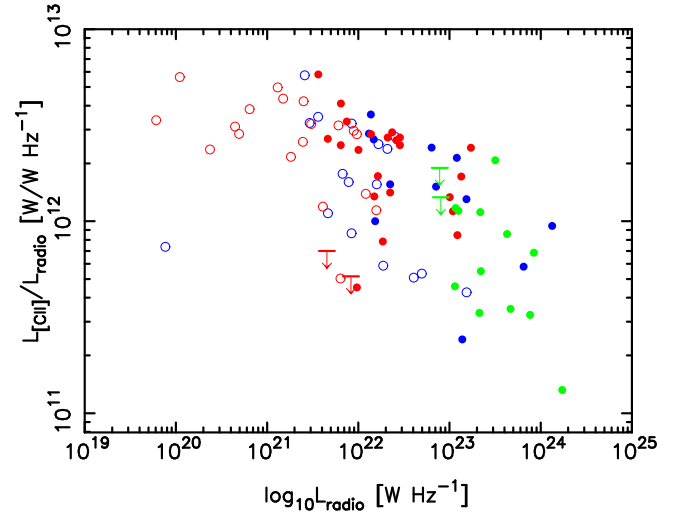


Fig. 12. As above, but normalising by the radio continuum luminosity.

Luhman et al., 2003), must also account for similar decreases as measured against the molecular gas and radio continuum luminosities.

3. Summary

In addition to the well documented drop in the $L_{\text{[CII]}}/L_{\text{FIR}}$ ratio with far-infrared luminosity in extragalactic sources, we find similar decreases with the molecular gas and radio continuum luminosities. This indicates that there is a [C II] deficit in relation to each of these properties, which due to the flux limited nature of the surveys, suggests a relative [C II] decline with luminosity. If evolutionary in nature, the order of magnitude decrease in the mean $L_{\text{[CII]}}/L_{\text{FIR}}$ ratio over the past 12% of the history of the Universe, could be due to a decrease in the metallicities, although, as per some of the literature, we see no evidence of this. The decline in $L_{\text{[CII]}}/L_{\text{FIR}}$ is, however, dominated by the ULIRGs at redshifts of $z \sim 0.1$ as well as the two QSOs, at $z = 4.69$ and 6.42 , and so rather than a detectable evolutionary effect, the decreasing $L_{\text{[CII]}}/L_{\text{FIR}}$ ratio is more likely the cause of a change in the demographics of the objects which can be detected at these distances.

We suggest that the excess FIR and radio luminosities arise from additional AGN activity, where the former is the result of dust in the embedded circumnuclear torus being heated by ultra-violet photons, in addition to the underlying ultra-violet emission from the stellar population. Both Negishi et al. (2001) and Luhman et al. (2003) also advocate non-PDR mechanisms as being responsible for some of the far-infrared emission. Furthermore, if the radio emission was due to the same ionised gas as traced by the [C II] emission, we would not expect a relative decrease in $L_{\text{[CII]}}/L_{\text{radio}}$. This may also be indicative of an increasing AGN contribution to the luminosity of these objects and towards the high end (i.e. the ULIRGs of Luhman et al. 2003), these sources would be considered radio galaxies.

Whether caused by an embedded AGN or vigorous star forming activity, the heating of the dust is the most likely explanation for the decrease in the [C II] luminosity in relation to that of the FIR. So although the gas is not expected to be heated by quite the same extent as the dust, the changing galaxy types, as traced by the increasing luminosities, may imply different cooling mechanisms. One possibility is an in-

crease in the relative contribution of the cooling by the [O I] line, which is known to become more dominant at higher ultra-violet fluxes (Kaufman et al., 1999), thus tracing the warmer dust (Malhotra et al., 2001). Furthermore, like the molecular gas and radio continuum luminosities, in comparison with the FIR, the [O I] also exhibits an excess over the [C II] luminosity, although this is also depleted for the ULIRGs. An additional coolant may therefore be the CO emission, in which the higher rotational transitions are found to rival the cooling by the [C II] line in one of the ULIRGs of the sample (Papadopoulos et al., 2007), with the two high redshift endpoints (for which these transitions have also been observed) exhibiting no FIR excess in relation to the CO. We may therefore expect the warm molecular gas to also be located in the torus from which the additional FIR luminosity is arising, with the cooler gas, as traced by the low excitation rotational transitions, located at larger radii. Beyond the torus, in the main galactic disk, is also where most of the cool neutral gas, as traced by the H I 21-cm absorption, is believed to reside (Curran & Whiting 2009 and references therein).

Observations of the higher rotational CO transitions in the ULIRGs could determine whether these could contribute to the cooling budget in these extreme FIR environments (due to starburst/AGN activity), where the [C II] emission is apparently lacking. As well as this, our suggestion that the relative decline in [C II] with FIR is due to a changing demographic, and any associated evolutionary effects, could be further tested by:

1. Radio flux measurements of the two high redshift sources. At $z = 4.69$ and 6.42 the 1.4 GHz continuum flux would be redshifted to 250 and 191 MHz, respectively. Both of these frequencies are accessible by the Giant Metrewave Radio Telescope, although such low frequencies could be subject to severe interference.
2. [O I] observations of these quasars in order to verify that the excess in this line over the [C II] line extends beyond the local ($z \lesssim 0.13$) galaxies.
3. Confirming the $L_{\text{[CII]}}/L_{\text{FIR}} \lesssim 10^{-4}$ limit in PSS 2322+1944 at $z = 4.12$, as referred to in Maiolino et al. (2005) [Benford et al., in prep.], but not since published.
4. Further observations of the [C II] transition at $0.1296 < z < 4.69$, filling in the redshift gap in the $L_{\text{[CII]}}/L_{\text{FIR}}$ –luminosity distance distribution (Fig. 2). At $z \gtrsim 1$, sub-millimetre observations would also cover the redshift range where star formation is expected to be most prevalent (Pei & Fall, 1995; Lilly et al., 1996). However, at $\gtrsim 400$ GHz these observations are difficult, requiring the very best atmospheric conditions.

Acknowledgments

I would like to thank the anonymous referee for their very helpful comments which significantly improved the manuscript, as well as Matt Whiting for commenting on an early draft. Also Matt Whiting again, as well as Michael Murphy, for the various C subroutines I utilise and Martin Thompson for debugging (my use of) these. This research has made use of the NASA/IPAC Extragalactic Database (NED) which is operated by the Jet Propulsion Laboratory, California Institute of Technology, under contract with the National Aeronautics and Space Administration. This research has also made use of NASA's Astrophysics Data System Bibliographic Service and ASURV Rev 1.2 (Lavalley et al., 1992), which implements the methods presented in Isobe et al. (1986).

References

- Aalto, S., Booth, R. S., Black, J. H., & Johansson, L. E. B. 1995, *A&A*, 300, 369
 Albrecht, M., Krügel, E., & Chini, R. 2007, *A&A*, 462, 575
 Barvainis, R. & Ivison, R. 2002, *ApJ*, 571, 712
 Bertoldi, F., Cox, P., Neri, R., et al. 2003, *A&A*, 409, L47
 Bolatto, A. D., Jackson, J. M., & Ingalls, J. G. 1999, *ApJ*, 513, 275
 Bolatto, A. D., Jackson, J. M., Israel, F. P., Zhang, X., & Kim, S. 2000, *ApJ*, 545, 234
 Boselli, A., Lequeux, J., & Gavazzi, G. 2002, *A&A*, 384, 33
 Claussen, M. J. & Sahai, R. 1992, *AJ*, 103, 1134
 Clegg, P. E., Ade, P. A. R., Armand, C., et al. 1996, *A&A*, 315, L38
 Condon, J. J. 1984, *ApJ*, 287, 461
 Cowie, L. L., Barger, A. J., & Kneib, J.-P. 2002, *AJ*, 123, 2197
 Crawford, M. K., Genzel, R., Townes, C. H., & Watson, D. M. 1985, *ApJ*, 291, 755
 Curran, S. J., Johansson, L. E. B., Bergman, P., Heikkilä, A., & Aalto, S. 2001a, *A&A*, 367, 457
 Curran, S. J., Polatidis, A. G., Aalto, S., & Booth, R. S. 2001b, *A&A*, 368, 824
 Curran, S. J., Polatidis, A. G., Aalto, S., & Booth, R. S. 2001c, *A&A*, 373, 459
 Curran, S. J., Webb, J. K., Murphy, M. T., & Carswell, R. F. 2004, *MNRAS*, 351, L24
 Curran, S. J. & Whiting, M. T. 2009, *A&A*, submitted
 Curran, S. J., Whiting, M. T., Wiklind, T., et al. 2008, *MNRAS*, 391, 765
 Dalgarno, A. & McCray, R. A. 1972, *Ann. Rev. Astr. Ap.*, 10, 375
 de Mello, D. F., Wiklind, T., & Maia, M. A. G. 2002, *A&A*, 381, 771
 Eckart, A., Cameron, M., Rothermel, H., et al. 1990, *ApJ*, 363, 451
 Elfhag, T., Booth, R. S., Höglund, B., Johansson, L. E. B., & Sandqvist, Å. 1996, *A&AS*, 115, 439
 Gao, Y. & Solomon, P. M. 1999, *ApJ*, 512, L99
 Gao, Y. & Solomon, P. M. 2004, *ApJ*, 606, 271
 Greve, A., Becker, R., Johansson, L. E. B., & McKeith, C. D. 1996, *A&A*, 312, 391
 Hainline, L. J., Scoville, N. Z., Yun, M. S., et al. 2004, *ApJ*, 609, 61
 Heckman, T. M., Blitz, L., Wilson, A. S., Armus, L., & Miley, G. K. 1989, *ApJ*, 342, 735
 Iono, D., Yun, M. S., Elvis, M., et al. 2006, *ApJ*, 645, L97
 Isobe, T., Feigelson, E., & Nelson, P. 1986, *ApJ*, 306, 490
 Kaufman, M. J., Wolfire, M. G., Hollenbach, D. J., & Luhman, M. L. 1999, *ApJ*, 527, 795
 Lavalley, M. P., Isobe, T., & Feigelson, E. D. 1992, in *BAAS*, Vol. 24, 839–840
 Lees, J. F., Knapp, G. R., Rupen, M. P., & Phillips, T. G. 1991, *ApJ*, 379, 177
 Leroy, A., Bolatto, A. D., Simon, J. D., & Blitz, L. 2005, *ApJ*, 625, 763
 Lilly, S. J., Le Fevre, O., Hammer, F., & Crampton, D. 1996, *ApJ*, 460, L1
 Luhman, M. L., Satyapal, S., Fischer, J., et al. 1998, *ApJ*, 504, L11
 Luhman, M. L., Satyapal, S., Fischer, J., et al. 2003, *ApJ*, 594, 758
 Madden, S. C., Poglitsch, A., Geis, N., Stacey, G. J., & Townes, C. H. 1997, *ApJ*, 483, 200
 Maiolino, R., Cox, P., Caselli, P., et al. 2005, *A&A*, 440, L51
 Malhotra, S., Kaufman, M. J., Hollenbach, D., et al. 2001, *ApJ*, 561, 766
 Mauch, T. & Sadler, E. M. 2007, *MNRAS*, 375, 931
 Metcalf, R. B. & Magliocchetti, M. 2006, *MNRAS*, 365, 101
 Mochizuki, K., Nakagawa, T., Doi, Y., et al. 1994, *ApJ*, 430, L37
 Negishi, T., Onaka, T., Chan, K.-W., & Roellig, T. L. 2001, *A&A*, 375, 566
 Omont, A., Petitjean, P., Guilloteau, S., et al. 1996, *Nat.*, 382, 428
 Papadopoulos, P. P., Isaak, K. G., & van der Werf, P. P. 2007, *ApJ*, 668, 815
 Pei, Y. C. & Fall, S. M. 1995, *ApJ*, 454, 69
 Pierini, D., Leech, K. J., Tuffs, R. J., & Volk, H. J. 1999, *MNRAS*, 303, L29
 Prochaska, J. X., Gawiser, E., Wolfe, A. M., Castro, S., & Djorgovski, S. G. 2003, *ApJ*, 595, L9
 Röllig, M., Ossenkopf, V., Jeyakumar, S., Stutzki, J., & Sternberg, A. 2006, *A&A*, 451, 917
 Sadler, E. M., McIntyre, V. J., Jackson, C. A., & Cannon, R. D. 1999, *PASA*, 16, 247
 Sage, L. J. 1993, *A&A*, 272, 123
 Sanders, D. B. & Mirabel, I. F. 1985, *ApJ*, 298, L31
 Sanders, D. B., Scoville, N. Z., & Soifer, B. T. 1988, *Astrophys. J.*, 335, L1
 Sanders, D. B., Scoville, N. Z., & Soifer, B. T. 1991, *ApJ*, 370, 158
 Sanders, D. B., Scoville, N. Z., Young, J. S., et al. 1986, *ApJ*, 305, L45
 Sargent, A. I., Sanders, D. B., & Phillips, T. G. 1989, *ApJ*, 346, L9
 Smail, I., Ivison, R. J., & Blain, A. W. 1997, *ApJ*, 490, L5
 Smith, B. J. & Madden, S. C. 1997, *AJ*, 114, 138
 Solomon, P. M., Downes, D., Radford, S. J. E., & Barrett, J. W. 1997, *ApJ*, 478, 144
 Solomon, P. M. & Sage, L. J. 1988, *ApJ*, 334, 613
 Spergel, D. N., Verde, L., Peiris, H. V., et al. 2003, *ApJS*, 148, 175
 Stacey, G. J., Geis, N., Genzel, R., et al. 1991, *ApJ*, 373, 423
 Strong, M., Pedlar, A., Aalto, S., et al. 2004, *MNRAS*, 353, 1151

- Tacconi, L. J., Tacconi-Garman, L. E., Thornley, M., & van Woerden, H. 1991, A&A, 252, 541
- Wiklind, T. & Henkel, C. 1989, A&A, 225, 1
- Windhorst, R. A., Miley, G. K., Owen, F. N., Kron, R. G., & Koo, D. C. 1985, ApJ, 289, 494
- Wright, E. L., Mather, J. C., Bennett, C. L., et al. 1991, ApJ, 381, 200
- Yao, L., Seaquist, E. R., Kuno, N., & Dunne, L. 2003, ApJ, 588, 771
- Young, J. S., Xie, S., Tacconi, L., et al. 1995, ApJS, 98, 219
- Zheng, W., Mikles, V. J., Mainieri, V., et al. 2004, ApJS, 155, 73